

# Insights on the one-pot formation of 1,5-pentanediol from furfural with Co-Al spinel-based nanoparticles as an alternative to noble metal catalysts

L. Gavilà<sup>[a]</sup>, A. Lähde<sup>[b]</sup>, J. Jokiniemi<sup>[b]</sup>, M. Constantí<sup>[a]</sup>, F. Medina<sup>[a]</sup>, E. del Río<sup>[c]</sup>, D. Tichit<sup>[d]</sup> and M.G. Álvarez<sup>\*[a]</sup>

**Abstract:** CoAl-spinel nanoparticles prepared by liquid-feed flame spray pyrolysis (L-F FSP) and activated by reduction at different temperatures were used to investigate the hydrogenation process of furfural (FA) under mild conditions. Reduction of the spinel at 500 °C resulted in high FA conversion and selectivity to furfuryl alcohol (FFA, 81% yield, in 1 hour). Reduction at higher temperatures (i.e., 700 and 850 °C) led to the direct formation of diols (i.e., 1,5-PeD and 1,2-PeD) from FA. The differences in activity are attributed to the formation of surface metallic cobalt nanoparticles upon reduction at high temperature. A maximum of 30% 1,5-PeD was yielded after 8 hours of reaction under the optimized conditions of 150°C, 30 bar of H<sub>2</sub> and with 40 mg of catalyst reduced at 700 °C. This is the first report on the direct catalytic conversion of furfural to 1,5-pentanediol with a non-noble metal solid catalyst.

## Introduction

The global concern about fossil fuel depletion is dramatically increasing. As an alternative, biomass exploitation for chemical production has been intensively targeted to overcome this distress. Commonly, the transformation of biomass sources is addressed by targeting a set of molecules that can be further transformed in already applicable compounds or offering a versatile range of applications, the so-called building blocks<sup>[1]</sup>. Among them, furfural (FA) is one of the few which nowadays is completely produced from renewable resources<sup>[2]</sup>. FA has an enormous potential for chemical synthesis, and its derivatives have been proposed either as fuels or monomers for biopolymers production<sup>[3–8]</sup>. Diols, which are among the most appreciated monomers<sup>[9]</sup>, can be produced *via* FA hydrogenation<sup>[10]</sup>.

FA hydrogenation was already reported over copper chromite in

1931 by Adknins and Connor. They reported quantitative conversion of FA to furfuryl alcohol (FFA), and afterwards, in a second reaction, 70% yield of 1,2-pentanediol (1,2-PeD) and 1,5-pentanediol (1,5-PeD) from FFA<sup>[11]</sup>. However, both copper and chromium are known for their toxicity and, consequently, the use of these catalysts is often dismissed.

Recently, great efforts are being done to achieve good yield of diols from FA using environmental benign catalysts. Commonly, two reaction pathways are employed for these reactions<sup>[9]</sup>. One proceeds *via* direct ring-opening of FFA, which is often preferred as starting material (Scheme 1, route I) to either form 1,2-PeD or 1,5-PeD or both. The second one combines hydrogenation of FFA to tetrahydrofurfuryl alcohol (THFA) followed by hydrogenolysis of THFA (Scheme 1, route II). Independently of which one is employed, FFA or THFA are usually chosen as starting reactant to obtain the diols.

Due to the high amount of competitive reactions that FA can undergo (Scheme 1), the direct use of FA as starting material remains a challenge. Xu et al. reported 1,5-PeD production from FA over platinum supported inverse Co-spinel, achieving ca. 35% yield of 1,5-PeD<sup>[12]</sup>. They claimed that Co<sup>3+</sup> acts as active site for adsorption and C=C bond cleavage, while Pt catalysed the following reduction steps. Also, Tomishige's group has intensively studied diols production from renewable sources and has successfully developed a two steps system. Using Pd-Ir-ReO<sub>x</sub>/SiO<sub>2</sub> as catalyst, they obtained the greatest yield of 1,5-PeD (71%) achieved from FA<sup>[13]</sup>. This system takes advantage of Pd-ReO<sub>x</sub> catalytic activity for FA hydrogenation into THFA, while Ir-ReO<sub>x</sub> catalyses the THFA hydrogenolysis selectively into 1,5-PeD. Despite the great potential of this bifunctional catalyst, the active sites are based on precious metals, which negatively impacts on the cost of this technology and limits its application in a biorefinery scenario.

Therefore, in recent years, more studies have been performed in order to develop non-noble metal catalysts for FA hydrogenation. For instance, Wu et. al. reported FA hydrogenation to form either FFA or THFA, over bimetallic CuNi nanoparticles (NPs) supported on Mg/Al oxides<sup>[14]</sup>. Using monometallic catalysts, Audemar et. al., have proposed Co NPs confined in a mesoporous material for practically quantitative hydrogenation of FA to FFA<sup>[15]</sup>. Lee et. al. successfully applied a Co supported on TiO<sub>2</sub> catalyst for continuous flow FFA hydrogenation in aqueous media, producing 30% of 1,5-PeD<sup>[16]</sup>. However, to the best of our knowledge there is no report of the one step production of diols from FA over non-noble metal-containing catalysts. In this regard, here, it is presented the activation and catalytic

[a] Dr. L. Gavilà, Prof. F. Medina, Dr. M. Constantí, Dr. M.G. Álvarez\*  
Department of Chemical Engineering  
University Rovira i Virgili  
43007 Tarragona (Spain)  
E-mail: mayra.garcia@urv.cat

[b] Dr. A. Lähde, Prof. J. Jokiniemi  
Department of Environmental and Biological Sciences  
University of Eastern Finland  
FIN-70211 Kuopio (Finland)

[c] Dr. E. del Río  
Independent researcher

[d] Dr. D. Tichit  
Institut Charles Gerhardt  
Univ. Montpellier, CNRS, ENSCM  
34296 Montpellier Cedex 5 (France)

behaviour of Co-Al spinel NPs synthesized by flame spray pyrolysis (FSP) in the one step one pot reduction of FA to PeDs. Metal oxide NPs synthesized via FSP present typically smaller crystalline size and higher surface areas than metal oxide catalysts prepared by conventional methods (e.g. precipitation or sol-gel). In addition, aerosol methods ensure a uniform metal dispersion in the catalyst<sup>[17]</sup>. These characteristics are highly desirable for heterogeneous catalysts. Activation of Co-Al spinel NPs was performed by reduction at different temperatures. The strong interaction between Co and Al species in the spinel may prevent the aggregation of Co in too large particles under the harsh reduction conditions, and will in turn improve stability and catalytic efficiency. A detailed characterization of the materials is presented as well as a systematic catalytic study for the direct conversion of FA to PeDs.

## Results and Discussion

### Preparation and characterization of catalysts

Co-Al spinel NP was prepared as described elsewhere<sup>[18]</sup>. The FSP system used for particle preparation has been described previously<sup>[19]</sup>. Briefly, the precursor solution (Co/Al molar ratio of ca. 0.22) was fed through a capillary at a rate of 5 mL/min and atomized with a high-pressure dispersion gas, O<sub>2</sub>, at a flow rate of 5 L/min. A premixed methane-oxygen flamelet with gas flow rates of 1 and 2 L/min, respectively, ignited the atomized precursor solution, resulting in the formation of a high-temperature flame, with temperatures exceeding 1700 °C. The produced particles were collected on a Teflon filter (Zefluor, Pall Corporation).

**Table 1.** Textural properties of as-synthesized and reduced Co-Al spinels and crystallite size of metallic Co produced upon reduction.

| Sample     | S <sub>BET</sub> (m <sup>2</sup> /g) | V <sub>p</sub> (cm <sup>3</sup> /g) | Average pore diameter (nm) | Crystallite size (nm) <sup>[a]</sup> |
|------------|--------------------------------------|-------------------------------------|----------------------------|--------------------------------------|
| CoAlO-as   | 174                                  | 1.21                                | 10                         | -                                    |
| CoAlO-r500 | 170                                  | 1.13                                | 10                         | -                                    |
| CoAlO-r700 | 139                                  | 1.12                                | 13                         | 2.8 ± 0.4                            |
| CoAlO-r850 | 112                                  | 0.68                                | 15                         | 9 ± 1                                |

[a] Average crystallite size calculated through Scherrer equation with integration of all the Co<sup>0</sup> diffraction planes using the double Voigt approach with Topas program. The instrumental resolution function has been estimated with LaB<sub>6</sub> (NIST 600a).

The textural properties of the Co-Al spinel catalysts were studied by N<sub>2</sub> adsorption at -196 °C. The N<sub>2</sub> adsorption-desorption isotherms of all the samples exhibited a type IV adsorption branch with a H3 hysteresis loop (upon the IUPAC classification<sup>[20]</sup>), (figure not shown), indicating the presence of aggregates of plate-like particles giving rise to slit-shaped pores. The BET surface area, total pore volume and average pore diameter of the cobalt aluminates are reported in Table 1. The as-synthesized (CoAlO-as) sample and that reduced at 500 °C

(CoAlO-r500) presented similar specific surface areas of ca. 170 m<sup>2</sup>/g and pore volumes of ca. 1.20 cm<sup>3</sup>/g. The specific surface area decreased with the increasing reduction temperature. It indeed dropped of about 36%, i.e. from 174 to 112 m<sup>2</sup>/g, between the as-synthesized sample and that reduced at 850 °C (CoAlO-r850). Concurrently, the pore volume decreased from 1.21 cm<sup>3</sup>/g to 0.68 cm<sup>3</sup>/g.

The XRD patterns of both the as-synthesized Co-Al NPs and of the reduced materials revealed the presence of spinel structure; however, it cannot be concluded whether they corresponded to normal (CoAl<sub>2</sub>O<sub>4</sub>), inverse (Co<sub>2</sub>AlO<sub>4</sub>) or Co<sub>3</sub>O<sub>4</sub> spinel, since all of them have the same crystalline structure (Figure 1). The diffractogram corresponding to the as-synthesized sample exhibited rather asymmetric peaks, suggesting the presence of several crystalline phases. To resolve the crystalline structure of this sample, the pattern was fitted using the double Voigt approach (by means of TOPAS program) using the structure cards of CoAl<sub>2</sub>O<sub>4</sub> (Fd-3m, JCPDS70-753), γ-Al<sub>2</sub>O<sub>3</sub> (Fd-3m, JCPDS79-1558), Co<sub>2</sub>AlO<sub>4</sub> (Fd-3m, JCPDS 38-0814) and Co<sub>3</sub>O<sub>4</sub> (F-3dm, JCPDS78-1969). Fitting (R<sub>wp</sub> = 7.57) revealed the coexistence of two cubic structures: γ-Al<sub>2</sub>O<sub>3</sub> and a Co-Al spinel (presumably Co<sub>2</sub>AlO<sub>4</sub>) with different lattice parameters (7.94 Å and 8.01 Å, respectively). Additionally, the Co/Al molar ratio in the precursor solution of approximately 0.22 was confirmed in the solid by EDX (see SI, Table S1 and Fig. S1), which is by far lower than the theoretical one in CoAl<sub>2</sub>O<sub>4</sub> and Co<sub>2</sub>AlO<sub>4</sub> of 0.5 and 2, respectively. Therefore, the formation of a Co-Al spinel and γ-Al<sub>2</sub>O<sub>3</sub> solid solution may be expected. However, further information was needed to confirm the type of spinel formed during the material synthesis.

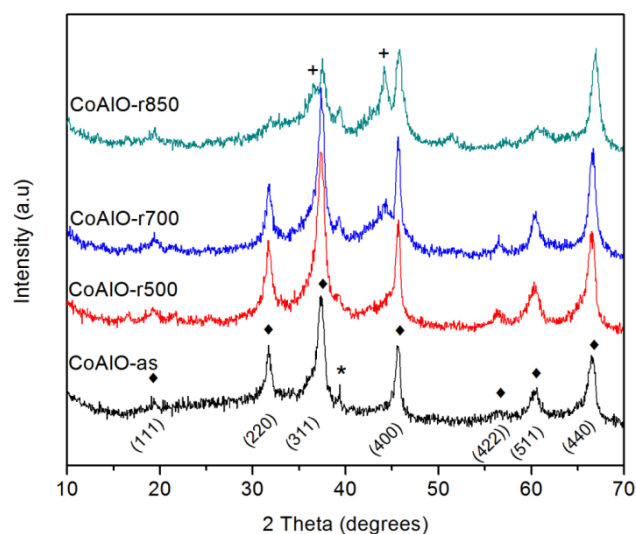


**Figure 1.** PXRD patterns of the as-synthesized sample and spinel reduced at different temperatures. (◆) CoAl-spinel; (\*) Al<sub>2</sub>O<sub>3</sub>; (+) metallic Co.

To allow such achievement, a Raman analysis of the as-synthesized sample was performed. Five main bands were observed at 192 (vs), 475 (m), 515(w), 614(w), and 683 (vs) cm<sup>-1</sup> (Figure 2). According to Mwenesongole<sup>[21]</sup> the presence of a band at 683 cm<sup>-1</sup> and the absence of a band at 408 cm<sup>-1</sup> might discard the presence of normal spinel (CoAl<sub>2</sub>O<sub>4</sub>). On the other hand, the blue-green colour of the sample might discard the

presence of  $\text{Co}_3\text{O}_4$  spinel having black colour. These features clearly suggest the presence of an inverse  $\text{Co}_2\text{AlO}_4$  spinel in the sample. Therefore, a large amount of  $\text{Al}_2\text{O}_3$  might be present according to the Co/Al molar ratio of ca. 0.22.

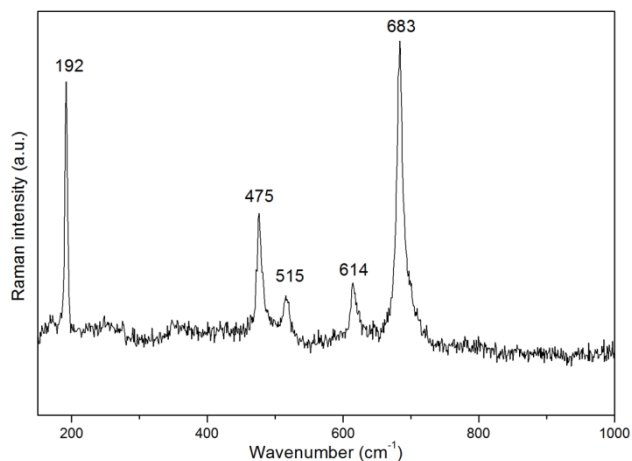


**Figure 2.** Raman spectrum of the as-synthesized  $\text{Co}_2\text{AlO}$  spinel at an excitation laser wavelength of 785 nm.

Upon sample reduction at increasing temperatures, several evolutions were observed in the XRD patterns (Fig. 1). Particularly, the relative intensity of the peaks at  $46^\circ$  and  $67^\circ$   $2\theta$  corresponding to 400 and 440 planes of a cubic structure, respectively, increased while that of the peaks at  $32^\circ$  and  $37^\circ$   $2\theta$  corresponding to 220 and 331 planes, respectively, decreased. Taking into account that  $\text{Co}_2\text{AlO}_4$  spinel and  $\gamma\text{-Al}_2\text{O}_3$  have both a cubic structure, these changes in intensity were tentatively attributed to the partial destruction of the crystalline structure of  $\text{Co}_2\text{AlO}_4$  spinel during reduction, while  $\gamma\text{-Al}_2\text{O}_3$  structure remained unaltered, hence increasing its relative intensity. Additionally, when the sample was reduced at 700 and 850  $^\circ\text{C}$ , new peaks developed corresponding to a cobalt bearing face centered cubic structure (Fd3m-(225) JCPDS 89-4307) as showed in Figure 1. This agrees with spinel degradation upon reduction at higher temperatures, segregating cobalt metal nanoparticles. Further, the intensity of the metallic Co peaks increased when the reduction temperature rose from 700 to 850  $^\circ\text{C}$  according to the growth of the particle size from 2.8 to 9 nm as established by XRD using the Scherrer equation (Table 1). It is also noteworthy that the crystallinity of the sample decreases as the reduction temperature increases suggesting formation of amorphous phase. This behavior was expected taking into account the deformation that  $\text{Co}_2\text{AlO}_4$  structure may suffer upon Co segregation from the crystal lattice.

TPR analysis gives information about the reduction process in the Co-Al spinel NPs and the changes in the structure. The TPR profile of the as-synthesized sample showed two major signals (Figure 3A). A small broad peak extending from 300 to 550  $^\circ\text{C}$  corresponded to the more reducible cobalt oxide species at the surface of  $\text{Co}_2\text{AlO}_4$  spinel or to the reduction in two steps of small amounts of  $\text{Co}_3\text{O}_4$  indiscernible by XRD. As previously reported, XRD analysis did not show the presence of metallic Co when the sample was reduced at 500  $^\circ\text{C}$ , which suggests the

absence of highly reducible CoO species in the sample. The second reduction peak of higher intensity in the 600-900  $^\circ\text{C}$  region exhibiting an asymmetric shape, suggested the presence of at least three different species in different coordinative environments. The peak centred at 675  $^\circ\text{C}$  could be attributed to the reduction of  $\text{Co}^{2+}$  formed in the first reduction step and/or present in the spinel, since XRD analysis already revealed metallic Co in that sample reduced at 700  $^\circ\text{C}$ . On the other hand, the shoulders at 760 and 870  $^\circ\text{C}$  could be attributed to the reduction of cobalt oxide species of low accessibility or strongly interacting with aluminium in the oxygen sublattice. This also agrees with the decrease in intensity of the  $\text{Co}_2\text{AlO}_4$  diffraction lines and the increase of those of metallic Co above 700  $^\circ\text{C}$ .

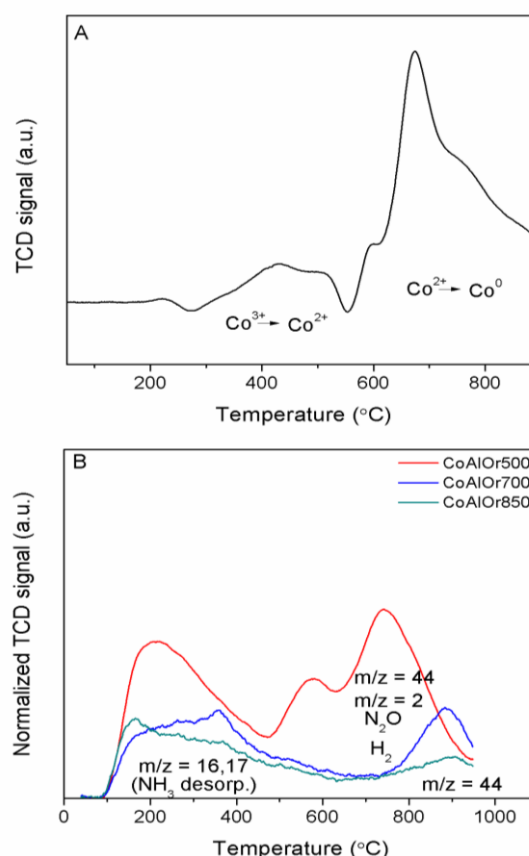


**Figure 3.** A) TPR profile sample for as-synthesized Co-spinel sample; B) TPD- $\text{NH}_3$  profile for CoAlO samples reduced at 500  $^\circ\text{C}$ , 700  $^\circ\text{C}$  and 850  $^\circ\text{C}$ .

**Table 2.** Results of TPD- $\text{NH}_3$  experiments on the Co-Al spinel reduced at different temperatures.

| Sample     | NH <sub>3</sub> desorption (mmol/g) |                                    | Total NH <sub>3</sub> <sub>des.</sub> evolved (mmol/g) | Acid sites density ( $\mu\text{mol}/\text{m}^2$ ) |
|------------|-------------------------------------|------------------------------------|--|---|
|            | (100-600 $^\circ\text{C}$ )         |                                    |  |   |
|            | W                                   | M-S                                |  |   |
|            | ( $\approx 200$ $^\circ\text{C}$ )  | ( $\approx 350$ $^\circ\text{C}$ ) |  |   |
| CoAlO-r500 | 0.89 (210)                          | --                                 | 0.89   | 5.2   |
| CoAlO-r700 | 0.48 (207)                          | 0.25 (377)                         | 0.73   | 5.3   |
| CoAlO-r850 | 0.27 (156)                          | 0.38 (326)                         | 0.65   | 5.8   |

In brackets: temperature maximum.

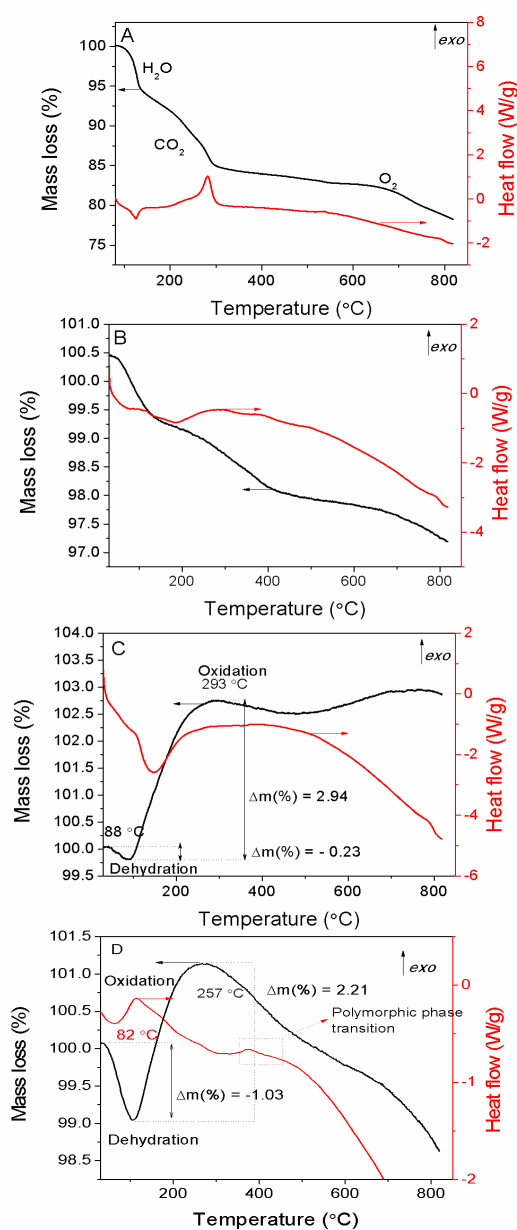
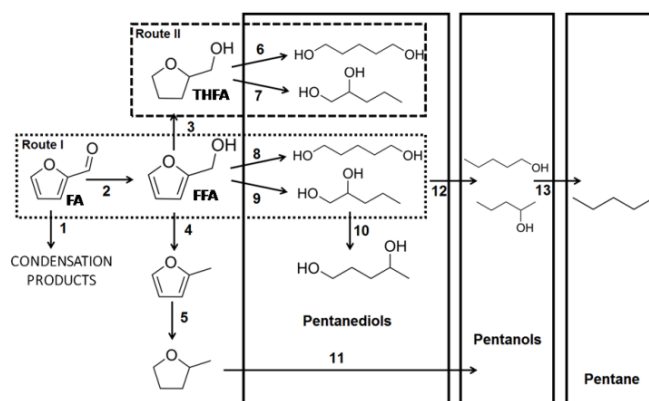


**Figure 4.** TGA analysis of A) as-synthesized CoAlO spinel nanoparticles; B) CoAlO spinel reduced at 500 °C; C) CoAlO spinel reduced at 700 °C and D) CoAlO spinel reduced at 850 °C.

It has been reported that the surface acidity of the catalysts plays a role on the selectivity in furfural hydrogenation<sup>[9,12]</sup> and on the hydrogenolysis ability of C-O bonds<sup>[9]</sup>. Hence, TPD-NH<sub>3</sub> coupled with mass spectrometry (MS) was monitored to calculate the concentration of acid sites at the surface after reduction *in situ* of the catalyst. The TPD profiles depended on the catalysts reduction temperature. Three main peaks were distinguished after reduction at 500 °C and two peaks after reduction at 700 and 850 °C (Figure 3B). Only the peak in the low temperature range, between 100 and 600 °C, corresponded

to desorption of ammonia, as evidenced by MS ( $m/z = 16, 17$ ), while the peak in the higher temperature range corresponded to desorption of ions with  $m/z = 44$ . This peak occurred at temperatures higher than 600 °C and its intensity decreased notably as the reduction temperature increased, which could suggest the presence of organic phase not completely burnt during synthesis. However, this assumption was completely discarded performing TG-MS analysis because CO<sub>2</sub> evolution occurred at lower temperatures (< 400 °C) (Figure 4A); then, any organic phase present in the as-prepared sample should be removed at 500 °C, the lowest reduction temperature used in the pretreatment of the spinel.

Notably, the contribution of the peaks corresponding to  $m/z = 44$  decreased when the reduction temperature increased and, interestingly, hydrogen evolution ( $m/z = 2$ ) was also detected, whereas N<sub>2</sub> evolution ( $m/z = 28$ ) was not observed. These features suggested that the peak at  $m/z = 44$  may correspond to N<sub>2</sub>O formed from NH<sub>3</sub> oxidation at the expense of the surface oxygen of the sample. This would also agree with the marked intensity decrease of this peak as the reduction temperature of the sample increases. Based on these results, the peak in the 100 to 600 °C range was used to calculate the amount of acid sites in the samples (Table 2). Its shape allows suggesting the existence of several components corresponding to acid sites with different strength. Deconvolution of peaks (see SI 2-4) revealed a single peak for the Co-Al spinel reduced at 500 °C, while the profiles of those reduced at 700 and 850 °C could be deconvoluted in two peaks with maxima at about 200 °C corresponding to weak acid strength (W) and 350-400 °C corresponding to medium-strong acid strength (M-S). The total concentration of acid sites (expressed as mmol of NH<sub>3</sub> desorbed per g of catalyst) gradually decreased with increasing the reduction temperature (Table 2). However, the amount of M-S strength acid sites increased with the increasing reduction temperature at expenses of the W acid sites. But the intrinsic strength of the M-S strength acid sites decreased when the reduction temperature increased from 700 to 850 °C because the maximum temperature of the corresponding peak shifted from 377 to 326 °C.



**Scheme 1.** Reaction pathways and products for the conversion of furfural.

### Catalytic performance in the FA reduction

The influence of the reaction temperature, catalyst loading and H<sub>2</sub> pressure, on the reduction of furfural (FA) was first studied with the Co-Al spinel catalyst reduced at 850 °C. Results are summarized in Table 3 and the evolution of conversion and product yields with time for all the reaction conditions are plotted in Figure 5 and the SI. Typically, the same general evolution of the curves of FA and product yields as a function of time was observed. FA concentration decreased rapidly with total conversion achieved in 2 – 4 h when the formation of FFA, which is the primary product, reached the maximum concentration. This latter further decreased due to formation of secondary by-products by hydrogenation (THFA) and/or hydrogenolysis (diols) of FFA. Scheme 1 shows some of the potential products that can be formed through FA hydrogenation.

The influence of the reaction temperature from 130 to 170 °C was studied with 40 mg of catalyst (10 wt%) and 20 bar of H<sub>2</sub> pressure. It had large impact in both the FA conversion and product yields. At 130 °C (Table 3, entry 2) the conversion of FA is ca. 58% after 8 h of reaction, achieving FFA production as only product with 48% yield (see also SI, Fig. S5A). At this temperature FFA did not suffer any consecutive hydrogenation or hydrogenolysis. At 150 °C complete FA conversion was achieved within 2 h (Table 3, entry 1, Fig. 5). As previously reported, FA reduction to FFA is rapidly achieved<sup>[9]</sup>. Afterwards, FFA is subsequently hydrogenated to form mainly tetrahydrofurfuryl alcohol (THFA) in a yield of 50.5%, remaining ca. 18% of FFA after 8 h of reaction. 1,5-pentanediol (1,5-PeD) in a yield of ca. 17% and slight amounts (1 – 2%) of 1-pentanol, 2-pentanol, and 1,2-PeD were also formed (Table 3, Entry 1). The products identified represent a mass balance of ca. 90% suggesting that pentane and/or condensed products were also present in low amounts.

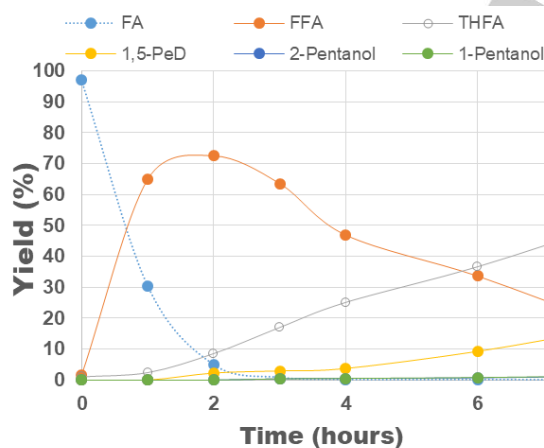


**Figure 5.** Products evolution with time in the FA reduction reaction with Co-Al spinel reduced at 850 °C. Reaction conditions: 150 °C, 20 bar H<sub>2</sub>, 40 mg catalyst.

The selectivity of products show that the reduction of the FFA furan ring (Scheme 1, step 3) was more favoured than its hydrogenolysis (Scheme 1, steps 8 and 9). Furthermore, if looking at the reaction products profiles it was observed that

FFA hydrogenation and FFA hydrogenolysis towards THFA and pentanediols, respectively, are parallel and competitive reactions (Figure 5), suggesting that THFA hydrogenolysis cannot occur or it does very scarcely (Scheme 1, steps 6 and 7). When the reaction was performed at 170 °C (Table 3, Entry 3, Fig. S5C), FA was totally reduced to FFA within 2 h. This latter was then subsequently reduced to produce a mixture of THFA, 1,2-PeD, and 1,5-PeD and pentanols. Here, it must be noticed that the mass balance of ca. 57%, point out that hydrogenation of the desired products to form pentanes (Scheme 1, steps 11 and 13) or even polymerization of FA (Scheme 1, step 1) must occur in larger extent than at 150 °C<sup>[9]</sup>. Indeed, some condensation products were detected, but not quantified. A remarkable feature is that, contrarily to what is generally reported for monometallic catalysts<sup>[15,22-24]</sup>, the Co-Al spinel-based catalyst reduced at 850 °C was able to produce 1,5-PeD from FA above 150 °C.

The influence of the catalyst loading in the range from 20 to 80 mg, i.e. from 5 to 20 wt%, was further examined at 150 °C under 20 bar of H<sub>2</sub> pressure (Table 3, entries 1, 6 and 7; Figure 4 and Fig. S5). Total FA conversion was in all cases obtained; however, the initial reaction rate increased along with the catalyst loading since total FA conversion was achieved in 1, 2 and 4 h, with loadings of 20, 10 and 5 wt%, respectively. Accordingly, the FFA yield after 8 h of reaction decreased from 50% to ca. 3% leading to increasing THFA and diols (1,2-PeD + 1,5-PeD) yields. However, it was noticeable that the mass balance of ca. 90% with 10 wt% of catalyst declined to ca. 75% for both 5 and 20 wt% of catalyst. The selectivity observed suggested that the non identified products were condensed products of FA with 5 wt% of catalyst and more likely pentanols and pentane formed by diols dehydration with 20 wt% of catalyst according to the larger amount of acid sites.

**Table 3.** FA conversion (C%) and reaction products yield (Y%) after 8 h at different reaction conditions with Co-Al spinel reduced at 850 °C.

| Entry | T (°C) | Wt <sub>cat</sub> (mg) | H <sub>2</sub> (bar) | FA (C%) | FFA (Y%) | THFA (Y%) | 1,5-PeD (Y%) | 1,2-PeD (Y%) | POL (Y%) |
|-------|--------|------------------------|----------------------|---------|----------|-----------|--------------|--------------|----------|
| 1     | 150    | 40                     | 20                   | 100     | 17.8     | 50.5      | 16.7         | 1.3          | 4.0      |
| 2     | 130    | 40                     | 20                   | 57.6    | 48.1     | --        | --           | --           | --       |
| 3     | 170    | 40                     | 20                   | 100     | --       | 20.8      | 14.4         | 8.7          | 12.7     |
| 4     | 150    | 40                     | 10                   | 99.1    | 68.2     | 4.7       | --           | --           | --       |
| 5     | 150    | 40                     | 40                   | 100     | --       | 68.7      | 24.2         | --           | 6.4      |
| 6     | 150    | 20                     | 20                   | 100     | 50.0     | 19.5      | 5.1          | --           | --       |
| 7     | 150    | 80                     | 20                   | 100     | 2.8      | 48.8      | 15.3         | 4.1          | 5.8      |
| 8     | 150    | --                     | 20                   | 23.5    | 22.7     | --        | --           | --           | --       |

FA: furfural; FFA: furfuryl alcohol; THFA: tetrahydrofurfuryl alcohol; PeD: pentanediol; POL: Pentanol (2POL+1POL)

The H<sub>2</sub> pressure was varied in the range from 10 to 40 bar with 10 wt% of catalyst at 150 °C (Table 3, entries 1, 4 and 5). There was in all cases total conversion of FA. However, the selectivity after 8 h of reaction varied. Under 10 bar of H<sub>2</sub>, FFA and THFA with 68.2 and 4.7% yield, respectively, were the only products obtained confirming that hydrogenation of the furan ring is easier than the hydrogenolysis of FFA. Hydrogenation of FFA was improved when the H<sub>2</sub> pressure increased, leading to 50.5 and 68.7% yield of THFA under 20 and 40 bar, respectively, and

hydrogenolysis also occurred. 1,5-PeD was indeed formed and its yield increased significantly from 16.7 to 24.2% when the H<sub>2</sub> pressure increased from 20 to 40 bar. Therefore, the higher 1,5-PeD yield was achieved under 40 bar of H<sub>2</sub> pressure with concurrently the highest 1-POL and 2-POL yields of ca. 6%, probably due to an increase in hydrogenation rates of the reaction steps 4 and 5 and/or subsequent hydrogenation of diols (Scheme 1). Moreover, in this case the mass balance was ca. 99% showing that no condensation or dehydration products were formed.

Finally, a blank test, without catalyst, was performed adding 2-propanol (IPA) and FA into the reactor pressurized with 20 bar of H<sub>2</sub> for 8 h and stirring at 150 °C. In this case, 23.5% of FA was converted forming ca. 23% of FFA (Table 3, entry 8), showing that hydrogenation of FA can be achieved in these reaction conditions; nonetheless, the low FA conversion pointed out the need of a catalyst for further FFA hydrogenation.

#### Influence of the catalyst temperature reduction

As previously mentioned, Co present in the spinel can be partially reduced and segregated from the crystalline structure when the reduction temperature is increased. We have also showed that the reduction temperature influences the surface area, the Co<sup>0</sup> crystallite size and the distribution of acid sites of the Co-Al spinel. All these structural changes were an incitement to study, the influence of the reduction temperature on the catalytic properties of the Co-Al spinel in the hydrogenation of FA. The study was performed at 150 °C with 40 mg of sample (10 wt%) under 20 bar of H<sub>2</sub> pressure (Table 4, entries 1-4).

The non-reduced Co-Al spinel was poorly active, leading to ca. 39% conversion and only primary FFA product formed after 8 h of reaction (Table 4, entry 2 and Fig. S7). After 2 h of reaction, total FA conversion was achieved with samples reduced at 500 and 700 °C. Whereas, 95% of FA conversion was obtained with sample reduced at 850 °C (Figs. S8 and S9). The sample reduced at 850 °C was less active and, in addition, led to the lower mass balance of ca. 72%.

When the catalyst was reduced at 500 °C, FFA was rapidly formed with a yield of ca. 80% after 1 h of reaction which then dropped to ca. 24% after 8 h. Further hydrogenation of FFA was rather slow, PeDs being obtained in a yield of ca. 6% after 8 h (Figure S8). The mass balance was low reaching ca. 57%. Although metal cobalt particles were not detected by XRD in the Co-Al spinel reduced at 500 °C, it was more active than without reduction (Table 4, entries 2 and 3). This means that the partially reduced cobalt species detected in the TPR experiment were able to achieve hydrogenation of FA into FFA and subsequently into THFA at a low rate.

Comparison of the product yields after 8 h of reaction for the catalysts reduced at 850 and 700 °C gave interesting trends (Table 4, entries 1 and 4, respectively). FFA was totally transformed with larger diols and pentanol yields at 700 °C than at 850 °C for a similar THFA yield of ca. 50% in both cases. The mass balance is slightly higher for reduction at 700 °C (82%) than at 850 °C (72.5%). Dehydration of 1,5-PeD to form alkenes and/or ethers that could not be monitored in our system,

although traces were detected in some cases by GC-MS, occurred more largely at 850 °C perhaps due to the low hydrogenolysis ability and the higher density of acid sites. This suggests that the first limiting step to obtain higher yields of PeDs is the hydrogenation rate of FFA. In this regard, the faster the FFA hydrogenation rate the higher the PeD yield.

**Table 4.** FA conversion (C%) and reaction products yield (Y%) after 8 h at different reaction conditions and catalyst reduction temperatures.

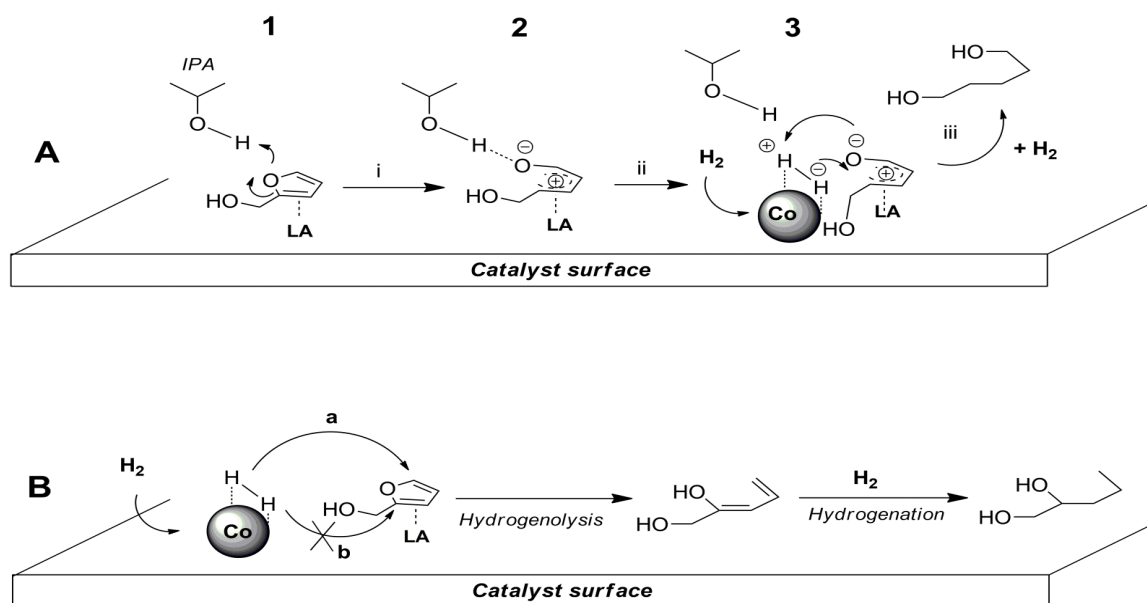
| Entry           | T <sub>red.</sub> (°C) | H <sub>2</sub> (bar) | FA (C%) | FFA (Y%) | THFA (Y%) | 1,5-PeD (Y%) | 1,2-PeD (Y%) | POL (Y%) |
|-----------------|------------------------|----------------------|---------|----------|-----------|--------------|--------------|----------|
| 1               | 850                    | 20                   | 100     | 17.8     | 50.5      | 16.7         | 1.3          | 4.0      |
| 2               | n.r.                   | 20                   | 38.9    | 38.9     | --        | --           | --           | --       |
| 3               | 500                    | 20                   | 100     | 23.7     | 27.4      | 4.7          | 1.4          | --       |
| 4               | 700                    | 20                   | 100     | --       | 50.4      | 22.0         | 3.3          | 6.6      |
| 5               | 700                    | --                   | 16.3    | 16.0     | --        | --           | --           | --       |
| 6               | 700                    | 30                   | 100     | --       | 62.2      | 29.8         | --           | 7.1      |
| 7               | 700                    | 40                   | 100     | --       | 57.0      | 12.5         | traces       | 2.5      |
| 8 <sup>1</sup>  | 700                    | 40                   | --      | --       | 42.1      | 40.3         | 1.8          | 10.5     |
| 9 <sup>2</sup>  | 700                    | 30                   | --      | --       | 94.7      | --           | --           | --       |
| 10 <sup>3</sup> | 700                    | 30                   | 100     | 96.4     | 2.9       | --           | --           | --       |

FA: furfural; FFA: furfuryl alcohol; THFA: tetrahydrofurfuryl alcohol; PeD: pentanediol; POL: Pentanol (2POL+1POL)

[1] Reaction starting from FFA instead of FA. [2] Reaction starting from THFA instead of FA. [3] Reused catalyst.

To get insights into the reaction mechanisms, FFA hydrogenation was performed at 150 °C, 30 bar and 40 mg of Co-Al spinel reduced at 700 °C (Table 4, entry 8). The reaction led to the formation of both THFA and 1,5-PeD in a similar yield, achieving a maximum of both yields of ca. 50% after 4 h. Further THFA and 1,5-PeD yields decreased slightly to ca. 40% after 8 h, to form further reduced products such as 1- or 2-pentanol. Notably, when looking at the reaction evolution (Figure S9), the formation profile of THFA and 1,5-PeD with time resulted rather similar. This confirms the previous suggestion that formation of 1,5-PeD occurs directly via hydrogenation of FFA instead of subsequent THFA hydrogenation. In this case, formation of 1,5-PeD from THFA seems to occur in a very slow rate or even not taking place.

To further confirm this hypothesis, the reaction was performed using THFA as substrate. Similarly to that reported by Xu et al.<sup>[12]</sup> with Pt-supported Co-spinel, our CoAl-spinel was not able to catalyse the THFA hydrogenolysis (Table 4, Entry 9). Thus, it seems that the mechanism of reaction entails the adsorption of the furanic ring of FFA on the acid surface of the Co-Al spinel from the double bond to be then opened and subsequently reduced (Scheme 2A). Further, the selective formation of 1,5-PeD vs. 1,2-PeD suggests that a Markovnikov carbocation is involved in the hydrogenolysis (Scheme 2A). Possibly, the hydrogenolysis needs the heteroatom activation by hydrogen bonding (step i), e.g. with solvent (IPA in this case). The carbocationic intermediate (2) may be stabilized by resonance of the furanic ring allowing, in step ii, the reaction of the hydrogen activated by the metallic Co NPs, which would be heterolytically dissociated (according to the proposed mechanism). Once the hydrogenolysis is achieved, standard double bond hydrogenation is produced followed by desorption of the reaction



**Scheme 2.** Proposed reaction mechanism for the formation of 1,5-PeD (A) or 1,2-PeD (B) from furfuryl alcohol. (IPA and LA stand for the solvent: 2-propanol and Lewis acid, respectively).

product (step iii). This hydrogenation seems to be very fast, since no double bond intermediates have been identified.

If the hydrogenolysis would start by attack of  $H_2$  to the furanic ring (Scheme 2B), it would take place by the less hindered carbon atom leading to mainly the 1,2-PeD isomer.

The improvement in the hydrogenation ability of the Co-Al spinel reduced above 500 °C was consistent with the presence of Co nanoparticles revealed by XRD. Their crystallite size increased from ca. 3 to 9 nm when the reduction temperature increased from 700 to 850 °C. In addition, TG analyses of the different reduced catalysts were performed to tentatively determine the amount of metallic Co in the catalyst from the mass gain produced through the oxidation of  $Co^0$  to  $Co_2O_3$  in air (Figure 4C and D). Samples were previously reduced *in situ* to avoid oxidation of the metallic Co by exposure to air during sample manipulation. Co-Al spinel reduced at 700 and 850 °C showed similar TG profile with gain of mass of about 2-3 wt%, corresponding to a ca. 6 - 8 wt% of metallic Co. That is, during the spinel reduction, about 6 wt% of the structural Co in the spinel is segregated forming metallic Co nanoparticles which are responsible of the hydrogenation activity. Notably, the amount of metallic Co in the sample calculated by TGA agrees with that obtained through calculations performed through Rietveld analysis of the XRD patterns (6.8 wt%). Therefore the Co-Al spinel catalyst reduced at 700 and 850 °C exhibited similar amounts of surface  $Co^0$  particles but of larger size at 850 °C. On the other hand, the sample reduced at 700 °C exhibited a lower rate of M-S acid sites but of higher intrinsic strength as shown by

TPD of  $NH_3$  (Table 2). FFA hydrogenolysis, which is related to the catalyst acid-base features, was produced in both cases when spinel was reduced at either 700 or 850 °C, but yield to PeD was higher with sample reduced at 700 °C. Having in mind the mechanism of reaction proposed above, the higher amount of PeD yielded by sample reduced at 700 °C would account for the higher surface acid strength that may provide better adsorption sites for furanic C=C bonds, likewise reported for alkenes<sup>[25,26]</sup>. Both  $Al^{3+}$  sites from alumina phases and, according to previous reports<sup>[12,27-28]</sup>,  $Co^{3+}$  cations from the  $Co_2AlO_4$  spinel phase could be responsible for the absorption of furfural; whereas, the higher dispersion of  $Co^0$  (based on its lower particle size, ca. 3 nm) favoured a rapid hydrogenation of intermediates..

#### Catalyst reuse

For the reuse test of the catalyst, the reaction was run at the optimal conditions (i.e. 150 °C, 30 bar and 700 °C as reduction temperature of the catalyst). Every 2 h (time in which total FA conversion is achieved), the reaction was stopped and cooled down and a new amount of FA and IPA was added to the reaction mixture. This protocol was repeated for 6 runs (Figure S10).

In all the 6 runs, the FA was converted within 2 h and FFA was continuously formed. However, further hydrogenation of FFA to either THFA or 1,5-PeD was produced only during the first two runs, achieving only 9% of THFA and 4% of 1,5-PeD, out of the total amount of added FA.

It is important to note that CoAl-spinel did not suffer any deactivation for FA reduction within the 6 runs. Thus, under semi-batch conditions it was found that FFA can be continuously and selectively produced from FA without any loss in activity, but neither THFA nor 1,5-PeD was formed after a second run. Hence, after a second test, the catalyst was neither able to hydrogenate the furan ring or catalyse hydrogenolysis of FFA. The activity towards PeD was not recovered upon catalyst washing with the solvent after a first reaction. Thus, to reactivate the catalyst towards the diol formation, a second type of reuse experiment was performed. A first reaction was carried out as usual at the optimal conditions. Once the reaction finished (8 h) the reaction was stopped, and the catalyst was washed, dried, calcined (300 °C) to remove any possible organic species adsorbed and re-reduced for a second run. During the second run, the catalyst was able to reduce all the FA, mainly forming FFA and ca. 3% of THFA (Table 4, Entry 9) but, again, no 1,5-PeD was detected, indicating a partial deactivation of the catalyst in spite of the reduction step prior its second usage.

Usually, one of the drawbacks of metallic catalysts, particularly in the case of Co-based catalysts, lies in the lack of stability. Possible deactivation routes can be sintering, re-oxidation of cobalt, formation of stable compounds between cobalt and the support, surface reconstruction, formation of carbon species on the cobalt surface, and poisoning. Therefore, regeneration addresses reversing the main deactivation processes by combustion, reduction and re-dispersion, respectively.

A previous hypothesis about the lability of these materials was based on the poisoning of the metallic active centres by adsorbed organic species or formation of carbon species; indeed, EDX analysis revealed a carbon content of ca. 9 wt.% in the used catalyst. Besides, carbon deposition may produce an increase of the specific surface area<sup>[29]</sup>, which would agree with measurements on the freshly reduced and used catalysts leading to 139 and 147 m<sup>2</sup>/g, respectively. However, the catalyst activity was not recovered upon combustion and re-reduction, suggesting a combined deactivation mechanism where more than one factor can be produced.

Leaching and sintering during liquid-phase reactions are intrinsic mechanisms of deactivation of metal catalysts. It is known that they come from the under-coordinated metal atoms at defects, corners, and edges<sup>[30,31]</sup>. Due to the preparation method and activation of these catalysts, it is expected that the material presents a high number of defects. Co leaching, if any, can be discarded through EDX analysis of the used catalyst, since no significant change of the Co/Al ratio was observed. This fact also suggests a strong metal-support interaction, revealing improved features in this material compared to other Co-based catalysts for liquid-phase conversion of biomass.

On the other hand, the PXRD pattern of the used sample revealed changes in the crystalline structure (Figure 6). Peaks corresponding to metallic Co still present were more intense in the used sample (CoAlO-r700 used) than in fresh catalyst, indicating an increase of crystallinity. Indeed, the crystallite size of the metallic Co increases from ca. 3 nm in the fresh catalyst to ca. 7 nm in the used one, which points to sintering of Co during the reaction. However, we cannot assure at this stage that the solely increase of crystallite size of the Co nanoparticles accounts for such deactivation.

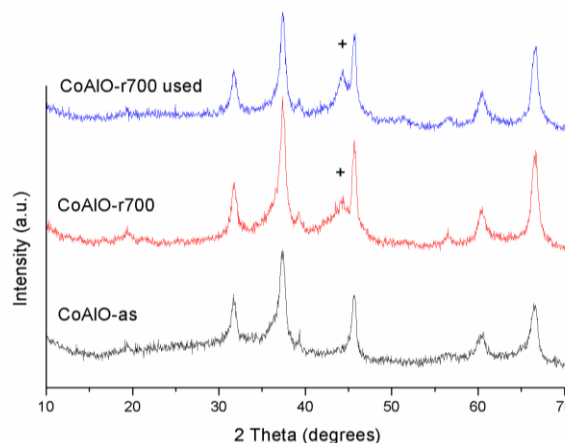


**Figure 6.** PXRD of the as-synthesized catalyst, catalyst reduced at 700 °C and catalyst after use. (+) metallic Co.

To gain further insights into the catalyst deactivation, the used material CoAlO-r700 was calcined at 300 °C and submitted to a new TPR cycle. It was found that the second reduction profile of the catalyst is completely different than the initial one. No reduction occurred, the consumption of H<sub>2</sub> starting at about 750 °C (Figure S11). Tentatively, this can be explained by a migration of Al<sub>2</sub>O<sub>3</sub> to the catalyst surface favoured by i) the Co sintering and ii) the liquid medium and the water generated during the reaction. This migration can lead to a restructuring of the Co NPs to form a core-shell structure of metallic Co covered by a cobalt-aluminate phase which would hinder the reducibility of the catalyst.

Thus, the deactivation seems to be most likely due to a combination of features such as carbon deposition, sintering of metallic NPs and bulk migration/surface transformation. But, though the different tests performed suggest an interplay of these factors, a comprehensive study needs to be performed.

## Conclusions

Most of the earlier published works for biomass conversion and specially for direct transformation of furfural towards 1,5-PeD are focused on the use of noble metal catalysts. However, for the sake of developing a more cost-effective and sustainable chemical industry it is required their replacement by affordable and abundant non-noble-metal catalysts. In this work we have demonstrated, for the first time, the activity of a non-noble metal CoAl-spinel based catalyst in the obtention of pentanediols directly from FA. These materials were able to achieve a 30% yield of 1,5-PeD from FA if the reaction conditions and catalyst reduction temperature are properly selected. The activity towards the hydrogenation/hydrogenolysis of FA was attributed to the surface acidity and growth of metallic surface Co nanoparticles segregated during reduction from the Co-Al spinel NP structure synthesized by flame spray pyrolysis. The formation of these Co nanoparticles strongly depended on the reduction temperature and have proved to be essential to



promote the FFA hydrogenolysis. Thus, a bifunctional mechanism has been proposed where the surface acid and metallic sites are involved and their distribution must be optimal for increasing 1,5-PeD yield.

This finding could be an important step for the design of new materials more stable and cheaper not only for the production of pentanediols from FA, but also for the selective production of FFA since these catalysts have proved to be stable for the FFA production and no metal leaching was detected. This fact suggests a strong metal-support interaction, revealing improved features in this material compared to other Co-based catalysts for aqueous phase conversion of biomass.

In summary, a nice strategy to prepare 1,5-PeD from FA without the need of precious metals is presented in this work. To the best of our knowledge, this is the first time that such fact is reported, which definitely opens a path to a new family of materials for biomass transformation; but further studies are still necessary to explore the mechanism of the catalyst deactivation and develop a better cobalt-containing catalyst which could enhance stability and selectivity.

## Experimental Section

### Catalyst synthesis

Co-Al spinel NP was prepared as described elsewhere<sup>[17]</sup>. Typically, aluminium acetylacetonate (Sigma-Aldrich) and cobalt acetate (Sigma-Aldrich) were used as received. The precursor solution consisted of a mixture of aluminium acetylacetonate (0.078 mol/L) and cobalt acetate (0.017 mol/L) dissolved in a solution containing 73 vol.% of methanol (J.T. Baker) in ion-exchanged water. The Co:Al molar ratio in the precursor solution was ca. 0.22. The flame spray pyrolysis system used for particle preparation has been described previously<sup>[18]</sup>. Briefly, the precursor solution was fed through a capillary at a rate of 5 mL/min and atomized with a high-pressure dispersion gas, O<sub>2</sub>, at a flow rate of 5 L/min. A premixed methane-oxygen flamelet with gas flow rates of 1 and 2 L/min, respectively, ignited the atomized precursor solution, resulting in the formation of a high-temperature flame, with temperatures exceeding 1700 °C. The produced particles were collected on a Teflon filter (Zefluor, Pall Corporation).

### Catalyst characterization

The X-ray diffraction (XRD) patterns of the Co-Al spinel NPs were recorded using a Siemens D5000 diffractometer (Bragg-Brentano for focusing geometry and vertical  $\theta$ - $\theta$  goniometer) with an angular  $2\theta$ -diffraction range between 5° and 70°. The sample was dispersed on a Si

(510) sample holder and spectra were collected with an angular step of 0.05° at 9 s per step of sample rotation. Cu K $\alpha$  radiation ( $\lambda=1.54$  Å) was obtained from a copper X-ray tube operated at 40 kV and 30 mA. Diffractograms were fitted using TOPAS software (V4.2, Bruker) to give a better understanding.

Specific surface areas were determined by N<sub>2</sub> adsorption at -196 °C using a Quantachrome Autosorb. Samples were previously degassed *in situ* at 200 °C under vacuum for 16 h. Surface areas were calculated using the Brunauer–Emmet–Teller (BET) method over a  $p/p_0$  range where a linear relationship was maintained.

Temperature-programmed reduction (TPR) experiments were performed in an Autochem II 2920 using 10% H<sub>2</sub> (30 mL/min) in Ar stream. The samples were heated from 30 to 950 °C with the heating rate of 5 °C/min. Before the reduction, the samples were heated in Ar flow at 200 °C for 1 h to remove physically adsorbed water.

Temperature programmed desorption (TPD) of NH<sub>3</sub> was conducted using an Autochem II 2920 instrument after reduction *in situ* at 500, 700 or 850 °C. Typically, ca. 100 mg of sample was pretreated *in situ* at 200 °C for 1 h to remove the physisorbed species on the surface. The NH<sub>3</sub> adsorption was performed with a flowing gas mixture containing 10% NH<sub>3</sub> balanced with Ar (30 mL/min) at 80 °C for 1 h. After adsorption, a flow of Ar (30 mL/min) was passed through the sample at 80 °C for 1 h to remove the physisorbed NH<sub>3</sub>. Then, the analysis was performed in flowing Ar (30 mL/min) from 40 to 950 °C (20 °C/min). Desorption was also followed by mass spectrometry to identify the species desorbed. The number of acid sites was calculated from the area under the NH<sub>3</sub> peak obtained through deconvolution of the TPD profiles using the equipment's software. The calibration of the instrument was done using injections of a known volume of 10% NH<sub>3</sub>-Ar gas mixture.

Thermogravimetric analysis (TGA) was carried out with a Sensys Evoanalyser from Setaram coupled with a MS spectrometer, under either Ar or air flow (20 mL/min), from room temperature to 850 °C, at a heating rate of 5 °C/min.

### Catalyst reduction

Typically, 40 mg of Co-Al spinel NP were reduced under dynamic conditions for 4 h in 5% H<sub>2</sub>-Ar mixture at 500, 700 or 850 °C with a heating rate of 5 °C/min.

### Furfural reduction reaction

Reduction of furfural (FA) was carried out in a 100 mL stainless steel autoclave (Autoclave engineers). Typically, a solution of 10 g/L of FA in 40 mL of 2-propanol (IPA) was placed in the reactor with 40 mg of catalyst previously reduced. Then the reactor was purged with hydrogen and pressurised at 20 bar (unless otherwise indicated). Once the desired temperature was reached, stirring was initiated (1000 rpm) and samples were withdrawn periodically to follow the reaction during 8 h.

Three different reuse experiments were carried out at the optimum conditions found. In the first semi-batch reuse set of experiments, the reaction was set as usual and each 2 h was stopped, the reaction vessel was depressurized, cooled down, opened, and 6 mL of IPA + 340  $\mu$ L of FA were added. This procedure was repeated 5 times for a total of 6 runs.

In the second reuse protocol, the reaction was run for 8 h, stopped and the catalyst was washed and reused for a second time.

In the third reuse protocol, the reaction was run for 8 h. Then, the catalyst was filtered and thoroughly washed with IPA, dried, calcined and reduced at 700 °C with 5% H<sub>2</sub>-Ar mixture prior reuse.

The products were identified and characterised with GC-MS. Calibration curves were performed using commercial standards of FA, FFA, THFA, 1-pentanol (2-pentanol calibration curve was assumed to be equivalent) and 1,5-pentanediol (1,2-pentanediol and 1,4-pentanediol calibration curves were assumed to be equivalent). Possible gaseous products formed such as pentane were not monitored in our system; however, the mass balance in most of the cases was in the range of 75–99%.

FA conversion and product yields were calculated on molar bases, typically:

$$\text{Yield of X (\%)} = \frac{C_x \text{ (mol/L)}}{C_{\text{FA}_0} \text{ (mol/L)}} \times 100$$

For the second recycling protocol, the yield was calculated over of the initial FA quantity; whereas for the semi-batch reuse protocol, the yield was calculated over the total FA added.

## Acknowledgements

This study was funded by the Spanish Ministry of Economy and Competitiveness (MINECO), project CTM2015-69848-R.

**Keywords:** furfural; 1,5,-pentanediol; hydrogenolysis; biomass; cobalt nanoparticles

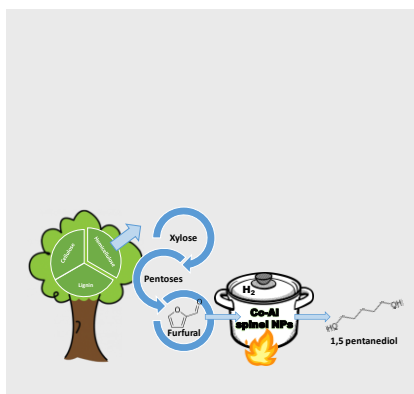
- [1] J. E. Holladay, J. F. White, J. J. Bozell, D. Johnson, T. Werpy, G. Petersen, A. Aden, Vol. II 2004, II.
- [2] R. Mariscal, P. Maireles-Torres, M. Ojeda, I. Sádaba, M. López Granados, *Energy Environ. Sci.* **2016**, 9, 1144–1189.
- [3] G. W. Huber, S. Iborra, A. Corma, *Chem. Rev.* **2006**, 106, 4044–4098.
- [4] A. Corma, S. Iborra, A. Velty, *Chem. Rev.* **2007**, 107, 2411–2502.
- [5] M. J. Climent, A. Corma, S. Iborra, *Green Chem.* **2014**, 16, 516.
- [6] J. C. Serrano-Ruiz, J. A. Dumesic, *Energy Environ. Sci.* **2011**, 4, 83–99.
- [7] P. Gallezot, *Chem. Soc. Rev.* **2012**, 41, 1538–1558.
- [8] S. G. Wettstein, D. Martin Alonso, E. I. Gürbüz, J. a. Dumesic, *Curr. Opin. Chem. Eng.* **2012**, 1, 218–224.
- [9] Y. Nakagawa, K. Tomishige, *Catal. Surv. from Asia.* **2011**, 15, 111–116.
- [10] D. Sun, S. Sato, W. Ueda, A. Primo, H. Garcia, A. Corma, *Green Chem.* **2016**, 18, 2579–2597.
- [11] H. Adkins, R. Connor, *J. Am. Chem. Soc.* **1931**, 53, 1091–1095.
- [12] G. L. W. Xu, H. Wang, X. Liu, J. Ren, Y. Wang, *Chem. Commun. (Camb)* **2011**, 3924–3926.
- [13] S. Liu, Y. Amada, M. Tamura, Y. Nakagawa, K. Tomishige, *Green Chem.* **2014**, 16, 617–626.
- [14] J. Wu, G. Gao, J. Li, P. Sun, X. Long, F. Li, *Appl. Catal. B Environ.* **2017**, 203, 227–236.
- [15] M. Audemar, C. Ciotonea, K. De Oliveira Vigier, S. Royer, A. Ungureanu, B. Dragoi, E. Dumitriu, F. Jérôme, *ChemSusChem* **2015**, 8, 1885–1891.
- [16] J. Lee, S. P. Burt, C. A. Carrero, A. C. Alba-Rubio, I. Ro, B. J. O'Neill, H. J. Kim, D. H. K. Jackson, T. F. Kuech, I. Hermans, *J. Catal.* **2015**, 330, 19–27.
- [17] D. P. Debecker, S. Le Bras, C. Boissière, A. Chaumonot, C. Sanchez, *Chem. Soc. Rev.*, **2018**, 47, 4112–4155
- [18] L. B. M.-L. Lähde, R. J. Chimentão, T. Karhunen, M. G. Álvarez, J. Llorca, F. Medina, J. Jokiniemi, *Adv. Powder Technol.* **2017**, 28, 3926–3306.
- [19] T. Karhunen, A. Lähde, J. Leskinen, R. Büchel, O. Waser, U. Tapper, J. Jokiniemi, *ISRN Nanotechnol.* **2011**, 2011, 1–6.
- [20] K. S. . Sing, D. W. Evert, R. A. . Haul, L. Moscou, R. A. Ierotti, J. Rouquerol, T. Siemieniowska, *Pure Appl. Chem.* **1985**, 57, 603–619.
- [21] A. E. Mwenesongole, A Raman- and XRD Study of the Crystal Chemistry of Cobalt Blue, University of pretoria, 2008.
- [22] O'Driscoll, J. J. Leahy, T. Curtin, *Catal. Today* **2015**, 279, 194–201.
- [23] X. M. X. Chen, L. Zhang, B. Zhang, X. Guo, *Sci. Rep.* **2016**, 28558.
- [24] P. N. Romano, J. M. A. R. de Almeida, Y. Carvalho, P. Priece, E. Falabella Sousa-Aguar, J. A. Lopez-Sanchez, *ChemSusChem* **2016**, 9, 3387–3392.
- [25] Jacques C. Védrine, Ioana Fechete, *Comptes Rendus Chim.* **2016**, 19, 1631–0748.
- [26] M. G. Álvarez, A. Urda, V. Rives, S. R. G. Carrazan, C. Martín, D. Tichit, I.-C. Marcu, *Comptes Rendus Chim.* **2018**, 21, 210–220.
- [27] C. Y. Ma, Z. Mu, J. Jun Li, Y. G. Jin, J. Cheng, G. Q. Lu, Z. P. Hao, S. Z. Qiao, *J. Am. Chem. Soc.*, **2010**, 132, 2608–2613.
- [28] S. Mo, S. Li, J. Li, Y. Deng, S. Peng, J. Chenab, Y. Chen, *Nanoscale*, **2016**, 8, 15763–15773..
- [29] P. R. de la P. J.M. Guil, N. Homs, J. Llorca, *J. Phys. Chem. B.* **2005**, 109, 10813–10819.
- [30] J. A. D. B. J. O'Neill, D. H. K. Jackson, A. J. Crisci, C. A. Farberow, F. Shi, A. C. Alba-Rubio, J. Lu, P. J. Dietrich, X. Gu, C. L. Marshall, P. C. Stair, J. W. Elam, J. T. Miller, F. H. Ribeiro, P. M. Voyles, J. Greeley, M. Mavrikakis, S. L. Scott, T. F. Kuech, *Angew. Chem.* **2013**, 52, 13808–13812.
- [31] G. W. H. J. Lee, D.H.K. Jackson, T. Li, R.E. Winans, J.A. Dumesic, T.F. Kuech, *Energy Environ. Sci.* **2014**, 7, 1657–1660.

## Entry for the Table of Contents

Layout 1:

## FULL PAPER

Furfural is one of the few chemical building-blocks only produced from agricultural sources (280 kTon/year). Its hydrogenation led to furfuryl alcohol and tetrahydrofurfuryl alcohol, while hydrogenolysis can produce 1,5-pentanediol, particularly interesting for its usage in polymer and resin synthesis. Co-Al spinel nanoparticles achieved the one-pot formation of such interesting compound.



L. Gavilà, A. Lahde, J. Jokiniemi, M. Constanti, F. Medina, E. del Río, D. Tichit and M.G. Álvarez\*

Page No. – Page No.

Insights on the one-pot formation of 1,5-pentanediol from furfural with Co-Al spinel-based nanoparticles as an alternative to noble metal catalysts